SMR/56 - 37

WINTER COLLEGE ON ATOMIC AND MOLECULAR PHYSICS

AND QUANTUM OPTICS

(23 January - 30 March 1979)

OPTICAL BISTABILITY: A TIME DEPENDANT ANALYSIS

P. Meystre
Max Planck Gesellschaft
zur Forderung der Wissenschaften E.V.
Projektgruppe für Laserforschung
Garching bei München
Fed. Rep. of Germany

OPTICAL BISTABILITY : A TIME DEPENDANT ANALYSIS +

P. Meystre

Max Planck Gesellschaft
Zur Forderung der Wissenschaften E. V.
Projektgruppe fur Laserforschung

ABSTRACT

A completely time-dependant analysis of optical bistability is presented. We first show that, dependant upon the relative scales of the atomic and field relaxation times, the system is driven either by the active medium (bad cavity limit) or by the electromagnetic field (good cavity limit). The transient response of the bistable system is qualitatively different in these two limits. We then discuss the concept of critical slowing down, and show which limitations it brings to the response time. We also discuss briefly its potentiel for device applications. These results are then applied to a case of particular practical interest, namely a bistable optical memory. We show that, although the nonlinear nature of the problem prohibits the use of standard theories, the response of the device to external noise can be largely understood in terms of intuitive arguments based on the results of a deterministic analysis.

+ Research supported by the Bundesministerium fur Forschung und Technologie and Euratom.
Lectures presented at the Winter College on Atomic and Molecular Physics and Quantum Optics, International Center for Theoretical Physics, Trieste, Italy 1979.

INTRODUCTION :

Under appropriate conditions, the light transmitted by an absorptive or dispersive medium placed inside an optical cavity can vary discontinuously and exhibit a hysteresis cycle. This effect, which is called optical bistability, has been predicted about ten years ago[1-3], and has been observed first by Gibbs, McCall, and Venkatesan[5], and later by a number of other groups[6-8]. This has led to much renewed interest in this problem. On the practical side, it presents numerous potential applications in optical data processing (optical memories, transistors, ...), pulse forming devices, etc... . Theoretically it also shows many fascinating aspects, since it is a beautiful example of the creation of an ordered structure far from thermal equilibrium.

These many facets under which optical bistability can be studied have made for an unusually wide spectrum of physicists and engineers working on it, and papers on optical bistability cover a whole range of interests, from elaborate non-equilitrium non-linear statistical mechanics to very down to earth device considerations.

Although this is somewhat of an oversimplification, the theoretical work on optical bistability can be divided into two subgroups. The first one is concerned mostly with the steady state aspects of the problem[4,9-13,15-17]. Here, the statistical properties of the system can be studied in great detail, and information on the spectrum of the scattered

light, for instance, may be obtained. Also, analogies may be drawn to other systems, (resonance fluorescence, chemical reactions, phase transitions, ...), leading to a better general understanding of non-equilibrium non-linear systems. It is important to note that we are concerned here with an optical system, for which many extremely accurate experimental methods are readily at hand. Thus, a quantitative verification of the theoretical predictions is much easier than, say, in the case of chemical reactions[20].

A second group a theoretical contributions is concerned mostly with time-dependant effects[6,9-11,14].However, the non-linear nature of the system makes the problem practically impossible to solve analytically in closed form, and one is forced to one of two approaches: either a linearized time-dependant analysis, or a numerical study of the problem. As the time-dependant response is obviously crucial for potential device applications, one does not expect linearized analyses[9-11] to be quite sufficiant. However, they are very important in that they suggest scaling laws which hopefully are still valid in the completely time-dependant problem. But one eventually has to make ones hands dirty and require the help of ones favorite computer.

This paper is concerned precisely with this last aspect of the theory of optical bistability. The primary question that we address here is to determine what are the crucial parameters which determine the switching of an optical bistable device form one branch to the other.

There are several ways to approach this problem, which have to do with how accurately one wishes to describe a given system. If one is interested in determining general scaling laws, it is better to limit the analysis to the simplest possible situation which still presents all the key characteristics of optical bistability. One obtains then numerical results which do not have too much quantitative relevance, but which should apply to a large class of devices. It is always possible to later on improve the model to obtain the hard numbers needed by the experimentalist next door.

In Section 2, we discuss briefly the model that we have used in our numerical work, and summarize the key results of the steady-state analysis which we will need.

We then proceed in Section 3 by analysing the response of the system to a step function incident field. This leads naturally to the distinction between the so-called good cavity and bad cavity limits of optical bistability.

The effects of critical slowing down, which can also be observed in the response to a step-function incident field, are the subject of a separate discussion in Section 4. A simple physical picture of this effect is presented.

In Section 5, we illustrate these results for a system of practical interest, namely a bistable device operated as a memory. Here, we also analyse the effects of external noise superimposed to the driving field. Although the analysis becomes in principle very complex in this case, we show that the dynamics of the system can still be largely understood

in terms of intuitive arguments based on the results of the deterministic analysis.

Finally, Section 6 is a summary and conclusion.

SECTION 2 :

We discuss optical bistability in terms of a simple model which has been analyzed first by Bonifacio and Lugiato[9]. Here, the active medium is described as an ensemble of two-level atoms placed inside a Perot-Fabry cavity and illuminated by an incident laser field. We assume that the atoms and the incident field are resonant, and also that a mode of the cavity is at the same frequency. This is what is called absorptive bistability, as opposed to dispersive bistability, where no resonance condition is assumed.

There are a few problems associated with considering such a model. The most bothersome is that up to now, most experiments have been concerned with dispersive bistability[5-8]. The reason for that is quite straightforward, namely that it is much easier to obtain optical bistability in a dispersive medium. This has to do with the fact that absorptive bistability requires the bleaching of an absorber, which takes a considerable amount of energy, while dispersive bistability involves a change in index of refraction, which does not require any absorption of energy and can be achieved at quite low powers.

However, absorptive bistability has several theoretical advantages which, at least for a first study, largely compensate its pitfalls. First, this is a relatively straightforward generalization of the problem of resonance fluorescence, which has been extensively studied recently. Second, one can take (in the semi-classical approximation)

the electromagnetic field to be real, which saves a considerable amount of computer time.

Absorptive optical bistability can be understood quite simply in terms of the following argument: if the incident field is very weak, the two-level atoms absorbe it, and essentially nothing is transmitted. The situation remains unchanged until the incident field is made strong enough to bleach the medium, at which point the system becomes transparent, with a consecutive abrupt increase of the transmitted light. The key to understand bistability is to realize that there is then a considerable amount of optical energy stored inside the cavity, and whose sole purpose is to keep the absorber bleached. The trick is that when one decreases the incident field, all this energy can keep the absorber bleached for weaker incident fields than on the way up. Clearly, however, this bleached regime can not be sustained for arbitrarily small fields, so that the transmitted field eventually jumps back down to the absorbing characteristics. However, the net result is a hysteresis cycle of the transmitted light as a function of the incident field, as schematically illustrated on Fig. 1.

Since we are dealing with an absorber, we do not expect quantum fluctuations to play a very important role, and therefore, will describe the electric field classically. The problem can then be formulated mathematically using standard techniques as described for instance in Ref 21. The only difficulty here is that since the field bounces back and forth between the mirrors of the cavity, we do not have

a simple propagation problem. There are two components of the electric field propagating in opposite directions, as shown on Fig 2, and expressing it as usual in terms of a slowly varying amplitude, it reads:

$$\mathcal{E}(z,t) = E_F(z,t)\, e^{-i(\omega_0 t + k_0 z)} + E_B(z,t)\, e^{-i(\omega_0 t - k_0 z)} + cc \qquad (2.1)$$

As we shall see, this leads to considerable difficulties in the solution of the problem. Under certain circumstances, however, one can argue that the fields are homogeneous inside the cavity, and in this case the propagation effects can be neglected. This is the so-called mean-field approximation, and we will later discuss it in some more detail. An alternative approach, which considerably simplifies the structure of the equations, is to consider a ring cavity. In that case, there is only one direction of propagation, and the steady-state problem can be solved analytically in closed form, without having to neglect propagation effects. However, since most of the results that will be discussed later have been obtained in the mean-field limit, we will not consider the ring-cavity problem at all. Also, all of the experimental results up to now have been obtained with a Perot-Fabry cavity.

Let us go on and see how the atoms interact with the electromagnetic field. The interaction Hamiltonian is $V = \vec{\mathcal{E}}.\vec{r}$, and the evolution of the atomic density matrix is given by

$$\begin{cases} \dot{\rho}_{aa} = -\frac{i}{\hbar}\left[V_{ab}\rho_{ba} + c.c.\right] \\ \dot{\rho}_{bb} = -\gamma_{\parallel}\rho_{bb} + \frac{i}{\hbar}\left[V_{ab}\rho_{ba} + c.c.\right] \\ \dot{\rho}_{ab} = -(i\omega_0 + \gamma_\perp)\rho_{ab} + \frac{i}{\hbar}V_{ab}(\rho_{aa} - \rho_{bb}), \end{cases} \qquad (2.2)$$

where V_{ab} is matrix element of V between the atomic states, and $\gamma_{\parallel} = 1/T_1$ and $\gamma_\perp = 1/T_2$ are the usual two-level system decay rates. The electromagnetic field is governed by Maxwell's wave equation

$$\left(\frac{\partial^2}{\partial z^2} - \frac{1}{c^2}\frac{\partial^2}{\partial t^2}\right)\mathcal{E}(z,t) = \frac{4\pi}{c^2}\frac{\partial^2 P}{\partial t^2} \qquad (2.3)$$

The relevant atomic quantities are of course the polarization

$$D(z,t) = \frac{1}{2}\sum_{atoms}\left(\rho_{bb} - \rho_{aa}\right) \qquad (2.4)$$

and inversion

$$P(z,t) = \frac{1}{2}\sum_{atoms}\left(\rho_{ab} + \rho_{ba}\right). \qquad (2.5)$$

The algebra which leads to the equations of motion is straightforward, and need not be repeated here. The key trick is to expand the polarization and inversion as

$$P(z,t) \cong P_F(z,t)\, e^{-i(\omega_0 t + k_0 z)} + P_B(z,t) e^{-i(\omega_0 t - k_0 z)} + c.c.$$

$$D(z,t) \cong D_0(z,t) + \left[D_1(z,t)\, e^{-2ik_0 z} + c.c.\right] \qquad (2.6)$$

Performing the standard slowly varying amplitude approximation, we then obtain

$$
\begin{cases}
\dfrac{\partial E_F}{\partial t} - c\dfrac{\partial E_F}{\partial z} = -g' P_F \\
\dfrac{\partial E_B}{\partial t} + c\dfrac{\partial E_B}{\partial z} = -g' P_B \\
\dfrac{\partial P_F}{\partial t} = \dfrac{\mu'}{\hbar}\left(E_F D_0 + E_B D_1\right) - \gamma_\perp P_F \\
\dfrac{\partial P_B}{\partial t} = \dfrac{\mu'}{\hbar}\left(E_B D_0 + E_F D_1\right) - \gamma_\perp P_B \\
\dfrac{\partial D_0}{\partial t} = -\dfrac{\mu'}{\hbar}\left(E_F P_F + E_B P_F\right) - \gamma_\parallel (D_0 - N/2) \\
\dfrac{\partial D_1}{\partial t} = -\dfrac{\mu'}{2\hbar}\left(E_F P_B + E_B P_F\right) - \gamma_\parallel D_1
\end{cases}
\qquad (2.7)
$$

The notation is that of Bonifacio and Lugiato. D1 is the envelope of the part of the inversion whose rapid space variation goes as $2ik_0z$. It plays a very important physical role, since it couples the forward and backward waves in the cavity. μ' is the modulus of the atomic dipole moment, and

$$g' = \left(\frac{4\pi\omega_0}{V}\right)\mu' \qquad (2.8)$$

where ω_0 is the frequency of the driving field and V the volume of the cavity. (Note that the explicit dependance on the volume disappears if one expresses the atomic quantities in terms of density rather than number of atoms N.)

It is important to realize that the set of equations (2.7) is the result of a trunction, where all terms oscillating at a frequency higher than $2\omega_0$ have been neglected. Carmichael[17] has studied in detail the validity of this truncation, and has shown that it leads to errors on the output fields on the order of about 10%, typically. More

serious perhaps from a conceptual viewpoint, the truncation also gives a qualitatively incorrect spatial dependance of the backward field. Although Carmichael has developed a method of solution of the problem which, at steady-state, does not require a truncation, no such technique is available in the time-dependant case. We will therefore use the set of equations (2.7), keeping in mind that it gives qualitative results only. Note that for the case of a ring cavity, the coupled Maxwell-Schroedinger equations form a closed set, so that no truncation is necessary and the problem is considerably simpler.

The last thing that we have to do is to determine the boundary conditions of the problem. This does not present any particular difficulty, and we find

$$
\begin{cases}
E_T(t) = \sqrt{T}\, E_F(0,t) \\
E_B(0,t) = \sqrt{R}\, E_F(0,t) \\
E_F(L,t) = \sqrt{R}\, E_B(L,t) + \sqrt{T}\, E_I(t) \\
E_B(L,t) = \sqrt{R}\, E_F(L,t) + \sqrt{T}\, E_R(t)
\end{cases}
\qquad (2.9)
$$

Here, we have followed what seems to be a tradition in optical bistability by labeling z = L the input mirror and z = 0 the output mirror. E_I (E_T) is the incident (transmitted) field, and R ,(T =1 -R), is the reflection (transmission) coefficient of the mirrors.

We are now over with the mathematical modeling of absorptive bistability. Note that, despite a series of rather crude approximations, we are still confronted with a set of equations with is very difficult to handle, even

numerically. However, as already advertised, we have one last card to play ,that is, the use of the mean-field approximation. It has the great advantage of getting rid of the spatial dependance in Equ. (2.7), so that one is left with ordinary differential equations. The price that one pays for that is that all propagation effects are then neglected.

To perform the mean-field approximation, one proceeds by first integrating Equ. (2.7) over the length of the cavity. One obtains then integrals of the form

$$\overline{AB} = \frac{1}{L}\int_0^L dz\, A(z)B(z) \qquad (2.10)$$

where A could be for instance an electric field and B a polarization. The key point is then to realize that if the fields are very homogeneous along z, one can to a good approximation factorize the integral as

$$\overline{AB} \simeq \overline{A}\,\overline{B} = \frac{1}{L^2}\int_0^L dz\, A(z)\int_0^L dz'\, B(z') \qquad (2.11)$$

One is then left with a series of 6 ordinary differential equations which describe the dynamics of the spatial averages of the fields, polarizations, and inversions. Since we have by now lost all hopes of doing a clean theory, we may as well go a step further and assume that the forward and backward fields are equal. The number of equations is then reduced to 3, which ,after some cosmetic algebra, read

$$\begin{cases} \dot{s} = (\gamma/K)(xd - s) \\ \dot{d} = (-2\gamma/K)[xs + (d-1)] \\ \dot{x} = -[2Cs + (x-y)] \end{cases} \qquad (2.12)$$

where we use the dimensionless inversion d, polarization p, and fields x and y:

$$\begin{cases} d = \frac{2}{N}(\bar{D}_0 + \bar{D}_1) \\ s = \frac{2}{N}\sqrt{\gamma_\perp/\gamma_\parallel}\,\sqrt{3}\,\bar{P} \qquad (\bar{P}_F = \bar{P}_B \equiv \bar{P}) \\ x = \frac{\mu}{\hbar\sqrt{\gamma_\parallel\gamma_\perp}}\frac{E_T}{\sqrt{T}} \\ y = \frac{\mu}{\hbar\sqrt{\gamma_\parallel\gamma_\perp}}\frac{E_I}{\sqrt{T}} \end{cases} \qquad (2.13)$$

where $\mu = \sqrt{3}\mu'$. We have taken $\gamma_\parallel = 2\gamma_\perp \equiv 2\gamma$. K is given by

$$K = \frac{cT}{L(1+\sqrt{R})}, \qquad (2.14)$$

and is the inverse life-time of the field inside the cavity. Algebraically, it was introduced in the equations by the spatial integration and the use of the boundary conditions. C is the so-called bistability coefficient:

$$C = \frac{\alpha L}{2T}, \qquad (2.15)$$

where α is the absorption coefficient

$$\alpha = \frac{N\lambda_0^2\bar{\tau}_0^{-1}}{8\pi V\gamma_\perp} \qquad (2.16)$$

As we shall see later on, C is the only coefficient which determines the existence of bistability in the mean-field approximation. The dot expresses the derivative with respect to the dimensionnel time

$$\tau = Kt. \qquad (2.17)$$

Before going any further, let us make a few comments on the variables that we use in Equ. (2.12), and on the mean-field

approximation.

One expects intuitively the mean-filed approximation to be valid for highly reflecting mirrors, and this turns out to be true. However, this is not a sufficient condition, and it has been shown both for a Perot-Fabry[14] and for a ring cavity[9] that one also needs the absorption of the medium to be weak. Mathematically, the condition of validity of the mean-field approximation is[9]:

$$\begin{cases} \alpha L \to 0 \\ T \to 0 \end{cases} \qquad (2.18)$$

with

$$C \equiv \frac{\alpha L}{2T} = \text{constant} \qquad (2.19)$$

The domain of validity of the mean-field approximation is shown on Fig. 3, where we have plotted the value T_c of T for which the deviation between the results of equ.(2.7) and (2.12) reach 10%, at steady state. The mean-field theory is valid below the curve.

The reason behind all the effort invested in writing the equations of motion in dimensionless form is obviously to prepare a numerical study. Note that x and y are the Rabi frequencies of the transmitted and incident fields, divided by $\sqrt{\gamma_\perp \gamma_\parallel}\sqrt{T}$. Also, we have followed the convention of Bonifacio and Luqiato for the definition of the inversion, and its value is 1 (and not - 1 as usual) when the atoms are in the ground state (see Eq. 2.5).

To conclude this section, we briefly redetive the bistability state equation of Bonifacio and Luqiato, starting from Equ.(2.12). At steady state, all the

derivatives are equal to 0, and the resulting algebraic set of equations can be solved trivially to give the incident field y as a function of x:

$$y = x + \frac{2Cx}{1+x^2} \qquad (2.20)$$

This equation of state has two extrema for $C > 4$. When inverted, it gives then the celebrated S-curve of optical bistability, whose only stable branches are those with positive slope. This is summarized on Fig. 4, where all the important parameters which will be used in the remaining of this paper are also indicated.

SECTION 3 :

We are now in a position to analyze the transient behaviour of an optical bistable device. We limit our discussion to the mean-field limit, described by the set of equations (2.12). Also, since we are not particularly interested for now in the transition region between monostable ($C < 4$) and bistable ($C > 4$) behaviour, we chose to work well into the bistable domain, and thus, most of the results that we will present are for $C = 20$. When C is determined, one sees from Equ. (2.12) that we are left with two parameters only, namely K and γ.

There are no particular difficulties associated with the numerical solution of Equ. (2.12), and just about any standard integration routine will do. We have chosen to use a fairly elaborate one, the so-called GEAR routine[22]. It presents the advantage of having an automatically adjusted integration step, which makes for an optimum computation time. This becomes important when one is faced with the submission of hundreds of jobs, as is the case when the effects of external noise are studied.

We proceed by first analyzing the response of the system to a step-function incident field. At $t = 0$, the initial conditions are determined by the steady-state solution of Equ. (2.12),

$$\begin{cases} X_0 = X_0 \\ Y_0 = X_0 + \dfrac{2CX_0}{1+X_0^2} \\ d_0 = 1/(1+X_0^2) \\ S_0 = X_0/(1+X_0^2) \end{cases} \qquad (3.1)$$

and at $t = 0 + \varepsilon$, the incident field is switched to a new value Y_1 which takes the device on the upper bistability branch. On fig. 5 and 6, we show the result of such a computation for $K = 10\gamma$ and $K = 0.1\gamma$. Clearly, the transient behaviour of the device is qualitatively different for these two limits.

Let us first analyze the limit where $\gamma \ll K$. For short times, one observe a small bump of the transmitted electric field. This is a feature that we have obtained in all of our runs, and typically it is bigger if X_0 is initially close to zero than close to 1. It is due to the combined action of the filling of the cavity by the new electric field, which occurs on a time-scale on the order K^{-1}, and a change in polarization in the active medium (dotted line on Fig. 5.) After some time, the active medium is bleached, that is, the inversion goes to zero (dashed line on Fig 5). At this point, the atomic medium is transparent, and the transmitted field becomes essentially that of an empty cavity. Thus, the system jumps from the lower to the upper bistability branch. Fig 5 shows that this switching is not monotonic. Rather, there are oscillations in the transmitted field x, and it is easy to verify that they are precisely at the Rabi frequency $\sqrt{2\gamma Y_1}/2\pi K$, which are a characteristic of single atom dynamics.

Once the system reaches the regime of Rabi oscillations, it always behaves exactly in the same way, irdependantly of the initial conditions at $t = 0$. Thus, the switching is clearly over by then. It is then possible to define a "switching

time" t_s as, say, the time necessary to reach the first maximum of the Rabi oscillations.

Before discussing this switching time in detail, let us compare these results to the dynamics when $\gamma \gg \kappa$. Here, the qualitative response of the system is changed completely. The most obvious difference is that the switching from the lower bistability branch to the upper branch is monotonic, and there are no oscillations at the Rabi frequency. More importantly perhaps, if one forgets for a moment the funny delay for short times, one finds that the growth of the trarsmitted field is exponential, with time constant κ^{-1}. This is essentially independant of X_0 and C, for C not too close to 4. Thus, in this case, there is nothing reminiscing of atomic dynamics left. The cavity drives the bistable system completely.

For this reason, this last limit $\gamma \gg \kappa$ has been called the good quality cavity limit, as opposed to the bad cavity limit $\kappa \gg \gamma$. This is somewhat of an unfortunate nomenclature, as it seems to imply that a Perot-Fabry with highly reflecting mirrors (high-Q cavity) will lead to a dynamic of the type shown on Fig. 6. One should be aware that this is not necessarily the case, as the "good-cavity" limit is in fact a combined characteristic of the atoms and the cavity. In particular, one can at least in principle think of using two different types of atoms with a same cavity, and reach the two different limits.

The fact that there is no trace of atomic dynamics left in the good cavity limit is not surprising. Rather, it is a

general feature of systems where two subsystems evolve on very different time-scales. It can be shown in all generality that in this case, the slowly varying system drives the rapidly varying one. In theoretical physics jargon, one says that the rapidly varying variable follows adiabatically the other one, and it can be "adiabatically eliminated". One is then left with equations of motion containing only the slow variables, that is, the dynamics of the system is explicitely independant of the rapidly varying subsystem. This adiabatic elimination technique will be further used in the next section to discuss the critical slowing down.

We now return to the notion of switching time, and first analyse it in some more detail in the bad cavity limit. We proceed by first studying the effect of the initial state of the bistable device on the value of X_0. The results of these calculations are summarized on Fig. 7, where we have plotted t_s for various values of C, as x_0 goes from 0 to 1, that is, as the initial state ranges over all the lower bistability branch.

There is a dramatic change as C is varied from C = 10 (weak bistability) to C = 22 (strong bistability). This can qualitatively be understood if one remembers one of the key features of optical bistability, namely that in the lower branch, the atoms are driven <u>cooperatively</u> by the reaction field inside the cavity. it is this cooperativity which is the origin of bistability, and what differentiates weak (or no) bistability from strong bistability is how strongly the atoms cooperate. In a weakly bistable system, the atoms are

not "locked" together very strongly, and one can understand that it is easier then to switch to the upper branch. Thus, t_s must be smaller for C small. The second feature exhibited on Fig. 7 is that t_s reaches a maximum for $X_0 = \sqrt{2/C}$ (see Fig. 4). It then decreases monotonically as X_0 is further increased. At the present, we do not have a good explanation for this behaviour. We note, however, that for large C the shortening of t_s becomes significant, and it may be important for device applications. Unfortunately, as will be discussed in section 5, it may be difficult in practice to work close to the limit $X_0 = 1$, because we are then much more sensitive to external noise. Therefore, some trade-off between fast switching and reliable operation will have to be considered.

SECTION 4 :

Up to now, we have varied only the initial state of the bistable device, and have studied its response to a pulse which takes it well into the upper branch. In practice, one would like to operate a device with as weak a driving field as possible. Therefore, one is interested in studying the dynamics of the system for incident fields which barely take it above the critical point to the upper branch.

This question is further motivated by the linearized analysis which predicts the existence of a critical slowing down in the vicinity of the critical point. Physically, this means that if the system is taken slightly out of equilibrium, it will take an infinitely long time to return to it. This has of course potentially very important implications, since it may put limitations of the kinds of signals that can be processed in a bistable device. The question that we address here is therefore to determine in a completly time-dependant analysis to which extent the predictions of the linearized analysis will be realized in practice.

It is easily shown that the concept of critical slowing down applies equally to the good and bad cavity limits. However, the apparition of Fabi oscillations in the last case makes the interpretation of the results somewhat more complicated. For the sake of clarity and conciseness, we therefore limit our analysis to the good cavity limit. This presents the further advantage that in this case, we can adiabatically

eliminate the atomic variables, as discussed earlier. This leads to a particularly simple description of optical bistability, in which critical slowing down can be understood immediately in terms of a mechanical analogy.

We proceed by first presenting the results of our numerical analysis. Initially, the system is taken to be at steady-state with no driving field present:

$$X_0 = 0 \quad , \quad Y_0 = 0, \quad d_0 = 1 \quad , \quad S_0 = 0 \quad , \qquad (4.1)$$

and at $t = 0^+$, the incident field Y_1 is switched on. On Fig.8, we have shown the transmitted field as a function of time, for different values of Y_1 . In this example a bistability coefficient $C = 20$, and the mean-field limit have been used. As Y_1 becomes closer and closer to the critical point $Y_c \tilde{=} C + 1 \ (=21)$, one observes the apparition of a significant delay time t_D before the device switches from the lower to the upper branch of the bistability curve. (This is precisely the "funny delay" that we had chosen to ignore in section 3.) However, the remarkable feature is that once the switching is initiated, the transmitted field grows exponentially with time constant K^{-1}, independantly of Y_1 . (This strictly holds only for strongly bistable devices, that is $C \gg 4$. For C on the order of 4, the transient response is more complicated, and one does not obtain a simple exponential growth.)

The apparition of a large delay as $Y_1 \to Y_c$ can be understood simply in terms of a mechanical analogy. To show it, we proceed by first adiabatically eliminating the atomic variables. Technically, this is done by neglecting the time

derivatives of S and d in Eq. (2.12) in comparison with the relaxation terms:

$$\dot{S} \ll (\gamma/K)\, S$$
$$\dot{d} \ll (\gamma/K)\, d \ . \qquad (4.2)$$

The atomic equations reduce then to algebraic forms, which can be trivially substituted in the field equation . It reduces then to

$$\dot{X} = -\left(X - Y_1 + \frac{2CX}{1+X^2}\right). \qquad (4.3)$$

Note that at steady-state, we recover the bistability equation (2.20).

Eq. (4.4) can be formally reexpressed as

$$\dot{X} = -\frac{\partial U}{\partial X} \qquad (4.4)$$

where

$$U(X) \equiv \int \left(X - Y_1 + \frac{2CX}{1+X^2}\right) dX = \frac{X^2}{2} - XY_1 + C\ln(1+X^2) \qquad (4.5)$$

plays the role of a potential.

Eq. (4.4) also describes the motion of a marble in the potential $U(X)$. On Fig. 9, we have plotted $U(X)$ for various values of the parameter Y_1 . For $Y_1 < Y_c$, it presents two minima, corresponding to the two possible stable states (two bistability branches). As $Y_1 \to Y_c$, however, the first minimum becomes shallower and shallower, to finally disappear for $Y_1 = Y_c$. For $Y_1 > Y_c$, there is only one minimum left, which corresponds to the fact that there is only one state on the bistability curve. Clearly, for Y_1 larger than, but close to, Y_c , the system is initially on

a shoulder which is essentially flat. In this case, the analogy with the marble obviously shows that it takes an extremely long time for the system to leave this state and fall to the minimum of the potential $U(x)$.

There is a little bit of a semantic problem associated with the use of the term critical slowing down in the situation discussed here, since it usually refers to the a return to equilibrium. However, what we are considering here is clearly an other facet of the same effect, which also has to do with the disappearance of the first minimum of the potential at $U(x)$.

This picture obviously does not explain why, once started, the transition from the lower to the upper branch always occurs on a time-scale K^{-1}. We note, however, that a similar situation occurs in many non-linear problems, as for instance in superfluorescence, where the pulse-shape (non-linear regime) is by and large independant of the delay τ_D (linear regime).

Clearly, the apparition of a large delay is undesirable for device applications where a fast response time is desired. We note, however, that it will not present any major difficulties in practice, since it can be overcome by increasing the incident field by a few percent (at least in the application considered here). Furthermore, the second feature of the critical slowing down, namely the constant rise-time K^{-1}, suggests novel applications of optical bistability such as compact optical delay lines. Also, since the delay t_D depends strongly on the final value y_1 of the

incident field, (see Fig. 10), a measure of t_D is also a very sensitive measure of the incident field. Thus, optical bistability may be useful in the design of electric field to time converters and of electrometers. In this case, however, the problem of internal and external fluctuations will be of importance.

SECTION 5 :

Up to now, we have considered the response of an optical bistable system to a step-function incident field. In this section, we would like to become more specific and discuss a problem which is directly relevant for device applications. We will then show how the concepts that we have introduced up to now apply in this case.

The application that we have in mind is a bistable optical memory. The operation of the system in this configuration is illustrated on Fig 11. A CW incident laser field y_0, chosen such that the initial steady-state lies on the lower branch within the double-valued region of the characteristic curve, determines the operating point of the memory. If an appropriate light pulse $y_1(t)$ is then superimposed on y_0 at some time t_0, the memory will switch to the upper branch, and will remain there after the passage of the pulse.

Such a behaviour is illustrated on Fig. 12, where we have plotted the transmitted field for various amplitudes and width of the incident pulse. The first example on this figure shows that if the pulse is too short, the device does not react and remain on the lower branch. On the next two examples, we have considered longer pulses, but varied their amplitudes. In both cases, the memory is switched, with a rise-time k^{-1}. However, in the second case, where the pulse is just large enough to take the system over the critical point, there is a large delay time, characteristic of the critical slowing down discussed in the preceding

section. Note that although in the case of a step-function, an increase of a few percent in y_1 was sufficient to get rid of that effect, here, we have to increase the amplitude of the pulse y_s by about a factor of two to eliminate the delay. Thus the effects of critical slowing down are much more severe in this case.

In principle, one could also decrease t_D by increasing the cw level y_0. However, in practice, it is desirable to have a working point as far as possible from the critical point, so that the device is not overly sensitive to internal and/or external noise. (To quantify the expression "as far as possible", we will in the second part of this section analyse the influence of external noise on the dynamics of the device. The internal quantum mechanical noise, which is expected to have little influence since we are dealing with an absorber, will be ignored completely here.)

We proceed then by first determining in a systematic way what incident pulse characteristics are needed to throw the device. In the absence of noise, a necessary condition for the memory to switch is obviously that $y_0 + y_s > y_c$, where y_c is the critical point of the bistability curve. However, this condition is certainly not sufficient, as one expects intuitively that the memory will not react to very short pulses. This intuition can be confirmed numerically, as illustrated on the upper part of Fig. 12.

In order to determine the conditions under which the memory will be switched, we solve, numerically, the equations of motion of optical bistability, with y_s of the form

$A \cdot \exp(-(t-t_o)^2/\hat{t}^2)$. For simplicity, we consider only the good-cavity limit, since the absence of Fabi oscillations in this case makes it simpler to interprete the numerical results.

The results of our analysis are summarized in Fig. 13. We plot the minimum pulse width $\hat{t}_m$ necessary to switch the memory as a function of the pulse amplitude A, for various CW levels y_o. In this example, the bistability coefficient $C = 2\mathcal{C}$, so that $y_c \cong C + 1 = 21$. The other relevant parameters are $K^{-1} = 1$, $T_1 = 10$, $T_2 = 2.0$.

For $A >> y_c - y_o$, we find that the minimum pulse width $\hat{t}_m$ is given by the product $A \cdot \hat{t}_m = cst.$, which is indicative of a pulse area scaling law (or, alternatively, an energy per unit bandwidth scaling law). As A approaches $y_c - y_o$, this scaling ceases to hold, and it takes extremely long pulses to activate the bistable memory. This is again an effect of the critical slowing-down of the system in the vicinity of the critical point.

We next consider the case when external noise is superimposed on the incident signal. We add to the total field a real, stationary, and gaussian noise signal y_n, which is characterized by having $\langle y_n \rangle = 0$, and

$$\langle y_n(t)\, y_n(t+\tau) \rangle = I \cdot \exp(-|\tau|/t_c). \qquad (5.1)$$

I is, then, the noise power, and t_c is its correlation time. Not surprisingly, we find that the system invariably switches provided the criteria of Fig. 13 are met. It is, however, much more difficult to determine the finite probability of switching the memory in the absence of signal (i.e. we now consider $y_s = 0$).

Instead of a general tunneling theory++ based on the solution of the time-dependant Fokker-Planck equation [18-19], we have chosen to limit ourselves to the following, intuitive, determination of the response of the memory to noise. Consider a 'test' signal y_T given by

$$y_T = \frac{1}{t_f} \int_{-\infty}^{t} dt'\, y(t') \exp(-(t-t')/t_f) \qquad (5.2)$$

where t_f is the inverse bandwidth of the device. On the basis of the deterministic analysis, one expects intuitively that the noise will switch the memory if $t_f \cdot y_T(t)$ exceeds the area $\Theta = A \cdot \hat{t}_m$ given by Fig. 2. For a Gaussian process, this gives a 'mean tunneling time' (mean time taken by the noise to switch the memory) scaling approximately as

$$\langle t \rangle \sim t_f \exp(\Theta^2/t_c\, t_f I) \quad . \qquad (5.3)$$

The only unknown quantity in Equ. (5.3) is the filtering time t_f. It can be evaluated by computing the response of the optical memory to two pulses which are incapable of switching the memory when acting separately, but can activate it when they occur simultaneously. An estimate of t_f is then obtained by varying the delay between the pulses and determining for which maximum value the device can still

---

++There are two major difficulties associated with such an approach: in general, one expects the noise to have a finite bandwidth, so that the Fokker-Planck equation is non-markovian; even in the limit of white noise, optical bistability is such a highly non-linear problem that it is doubtfull if the time-dependant Fokker-Planck equation is amenable to an analytical solution.

be activated.

Although this delay depends to some extent upon the precise pulse characteristics, it turns cut tc be cn the crder of K^{-1} for a very wide range of pulses. This is actually not surprising, since K^{-1} is precisely the dcminant time-scale in the gccd quality cavity limit of cptical bistability , as discussed in Section 3. It is therefore reasonable to take the filtering time $t_f \cong K^{-1}$ in our estimate of the mean tunneling time <t>.

We have numerically tested Eq. (5.3) fcr various noise parameters I and t . The results are summarized on Table 1,where we have reported the numerical values of <t> and their ratios in columns three and four and the ccrresponding values obtained from Eq. (5.3) in columns five and six. In the last column, we have given the number cf ccmputer runs used in each case. For large enough noise levels, there is a remarkable agreement between the numerical results and the scaling relation Equ. (5.3). This is exhibited in the predicted and computed ratios, which always fall within 10% of each other. The systematic discrepency of a about a factor of twc in <t> itself is due to the fact that the noise can switch the memory only if it is in phase with the CW Laser. Hencr, one should nct ccunt the cccasions when y_o and y_n are cf opposite sign, so that the noise is effective only half of the time. Introducing this factcr of two converts Eq. (5.3) to an equality which is in remarkable agreement with the numerical results .

For the case with small noise power, Eq.(5.3) seems to

underestimate the tunneling time <t>. This result is, however, within the statistical accuracy of the computer experiment, since the distributicns cf the switching times are broad, i.e. The variances are on the order of <t> itself.

This is illustrated on Fig. 14, where an histogram of the switching times for the conditicns $y_0 = 20.3$, $t_c = 10^{-2}$, $I = 25.0$ have been drawn.

In conclusion, we have shown that the dynamics of a bistable memory in the presence of external noise can be largely understood in terms of intuitive arguments based on the results cf a deterministic analysis. Although our model is oversimplified, both in its descriptien cf the ncise, and of the memory, we dc not expect significant qualitative changes to occur in more realistic systems. We are presently initiating an analysis of dispersive optical bistability, where the noise will effect not cnly the amplitude, but also the phase of the incident field.

CONCLUSION :

In these notes, we have presented a few aspects of the transient dynamics of optical bistable devices. We have shown that despite the fact that this problem is not amenable to an analytical solution in closed form, numerical studies permit to achieve a good general understanding of its main features. Obviously, we have treated here a very idealized model, and we do not expect our results to be of much quantitative value. However, as we said in the introduction, this was not our goal. Rather, we were interested in general scaling laws, and, to this extent, the numerical analysis presented here has lead to usefull results in a surprisingly easy way.

Clearly, we have not exhausted the problems which one may want to address . The most obvious follow-up is a similar study of dispersive bistability. We are precisely pursuing such a study at the present. Here, we are mostly interested in analysing external noise which is both amplitude and phase modulated.This study was not possible in the model presented here, where all fields were taken to be real.

An other fascinating problem, that we are studying in collaboration with the Milan group, is that of self-pulsing in optical bistability. Under appropriate conditions,

higher order modes of the cavity may be excited and, instead of relaxing to steady-state, reach a limit-cycle behaviour. Such an effect may be very usefull for applications, and for this reason, we have initiated a systematic parameter study in order to improve on the results of linearized analyses. Although preliminary results show discrepencies in some regions, the analytical results seem to by and large predict the dynamics of the system.

Also very promising is the potential use of optical bistability in pulse-forming devices.Preliminary results have shown that pulse-shortening, discrimination, etc... are all possible in principle. We are planning to study this aspect of bistability in more details ,both theoretically and experimentally.

To conclude, I would like to mention an other problem of great importance in statistical mechanics, where the example of optical bistability may bring some light, namely the question of "multiplicative noise sources". In situations where the noise term (in the Langevin equation of motion) is multiplicative, the macroscopic characteristics of the system may be changed, i.e. the phase-transition may either disappear, or have a different threshold,etc... Although such systems are in general very complex, optical bistability is a simple example that one may be able to

solve "exactly" on the computer, thus getting some insight into this problem. The difficulty here is mostly to dream-up a realistic model where the internal noise is large enough to be of interest.

We hope that these few remarks have shown that there is some future not only in optical bistability, but also in the general numerical study of phase transitions and related phenomena.

Acknowledgments:

Much of the material presented here has been studied in collaboration with P. Bonifacio, who got me interested in optical bistability. The analysis of external noise was done together with F. A. Hopf. It is a great pleasure to thank many friends and colleagues for usefull and challenging discussions on the material of these notes, and in particular M. Gronchi, G. Lauchs, L. Lugiato, A. Quattropani, M. Sargeant III, D. F. Walls, and H. Walther. However, all the mistakes are mine.

REFERENCES :

1. A. Szöke, V. Daneu, J. Goldhar, and N. A. Kurnit, Appl. Phys. Lett. 15 , 376 (1969)

2. J. W. Austin and L. G. Deshazer, J. Opt. Soc. Am. 61 , 650 (1971)

3. E. Spiller, J. Appl. Phys. 43 , 1673 (1972)

4. S. L. McCall, Phys. Rev. A9 ,1515 (1974)

5. H. M. Gibbs, S. L. McCall and T. N. Venkatesan, Phys. Rev. Lett 28 , 731 (1976); T. N. C. Venkatesan and S. L. McCall, Appl. Phys. Lett 30 , 282 (1977)

6. T. Bischofberger and Y. F. Shen, Appl. Phys. Lett. 32 , 156 (1978) ; Optics Lett. 4 , 40 (1979)

7. P. W. Smith, E. H. Turner, and P. J. Maloney, IEEE J. Quant. Elec. QE14 , 207 (1978)

8. D. Grischowsky, J. Opt. Soc. Am. 68 , 641 (1978)

9.R. Bonifacio and L. Lugiato, Opt. Commun. 19 ,172 (1976) ;Phys. Rev. A18 , 1129 (1978) ; Lett. Nuovo Cimento 21 , 505 (1978) ; Lett. Nuovo Cimento 21 ,510 (1978) ; Lett. Nuovo Cimento 21 ,517 (1978) ; Phys. Rev. Lett 40 , 1023 (1978); R. Bonifacio, M. Gronchi and L. Lugiato, Phys. Rev. A18, 2266 (1978); M. Gronchi and L. Lugiato, Lett. Nuovo Cimento (1979), to be published

10. H. J. Carmichael and D. F. Walls, J. Phys. B10 , L685 (1978); D. F. Walls, P. D. Drummond, S. S. Hassan and H. J. Carmichael, Proceedings of the Oji Seminar On Nonlinear Nonequilibrium Statistical Mechanics (Kyoto, July 1978) , to be published in Progress in Theoretical Physics; S. S.

Hassan, P. D. Drummond and D. F. Walls, Optics Commun 27 , 480 (1978); S. S. Hassan and D. F. Walls, J. Phys. A11 ,L87 (1978) P. D. Drummond and D. F. Walls, Optics Commun. 27 , 160 (1978)

11. L. M. Narducci, R. Gilmore, D. H. Feng and G. S. Agarwal, Opt. Lett. 2 , 88 (1978); G. S. Agarwal, L. M. Narducci, R. Gilmore and D. H. Feng , Phys. Rev. A18 , 620 (1978)

12. F. S. Felber and J. H. Marburger, Appl. Phys. Lett. 28, 731 (1976); J. H. Marburger and F. S. Felber, Phys. Rev. A17, 335 (1978)

13. C. R. Willis, Opt. Commun. 23 , 151 (1977)

14. P. Meystre, Optics Commun. 26 , 277 (1978); R. Bonifacio and P. Meystre, Optics Commun. 27 , 147 (1978); R. Bonifacio and P. Meystre, Optics Commun. to be published

15. A. Schenzle and H. Brand, Optics Commun. 27 ,485 (1978)

16. F. Schwendimann , J. Phys. A12 , L39 (1979)

17. H. J. Carmichael, preprint

18. H. A. Kramers, Physica 7 ,284 (1940)

19. R. Landauer, J. Appl. Phys. 33 ,2209 (1962)

20. On the subject of multistable chemical reactions, see for instance K.J. McNeil and D.F. Walls,J. Stat. Phys. 10 ,439 (1974)

21. M. Sargent III, M.O. Scully, and W.E. Lamb, Jr., Laser Physics ,Addison-Wesley, (1974)

22. A.C. Hindmarsh, GEAP ,Ordinary Differential Equations System Solver, LLL University of California document No UCID-3001 ,Rev.3 (1974)

FIGURE CAPTIONS :

Figure 1 :
Typical bistability curve, showing the hysteresis cycle in the transmitted field as a function of the incident field.

Figure 2 : Field configuration in a Perot-Fabry cavity. E_I = incident field, E_T = transmitted field, E_F = forward field, E_B = backward field, E_R = reflected field.

Figure 3 : Solid line: critical transmission coefficient below which the exact and mean-field theories agree within 10%, as a function of C. The dashed part of this curve corresponds to the onset of bistability, which is a stronger condition for small C. Dotted line: corresponding value of αL , obtained from Eq. (2.15).

Figure 4 :
Bistability curve x(y) for $C = 20$. the position of the initial and final states y_0 and y_1 are shown, as well as $y_c = C+1$ and $x_m = \sqrt{\frac{2}{C}}$.

Figure 5 :
Solid line : transient response of the transmitted field x(t) to a switch of the driving field from $y_0 = 13.8$ to $y_1 = 25.0$, for $C = 20$, $\gamma = 10K = 10$, $T = 5\%$. Dotted line: polarization s(t). Dashed line: inversion d(t).

Figure 6 :
Transient response of the transmitted field x(t) to a switch of the driving field from $y_0 = 13.8$ to $y_1 = 25.0$, for the same conditions as Fig. 5, but $\gamma/K = 0.1$. The time is in units of K^{-1}.

Figure 7 : Switching time t_s (in units of κ^{-1}) as a function of x_0, for C =10, 20, 22, and γ/κ = 10.0 (bad cavity limit).

Figure 8 :

Transient response of the transmitted field x(t) for various values of the incident field y_1, and C = 21.0. Mean-field theory, good cavity limit, time in units of κ^{-1}.

Figure 9 : Potential U(x) from Eq. (4.5) for various values of y_1 around the critical point y_c. Note the disappearance of the first minimum as $y_1 \to y_c$.

Figure 10 :

Delay time (in units of κ^{-1}) as a function of y_1. C =20.0, good cavity limit (γ =10κ), mean-field theory.

Figure 11 :

Memory operation of a bistable device: The characteristic bistability curve of the upper right quadrant shows the transmitted field x as a function of the incident field y, and exhibits the usual hysteresis. The lower right quadrant gives the incident field as a function of time, and the upper left quadrant the corresponding transmitted field, also as a function of time.

Figure 12 : response of the bistable memory to the superposition of a gaussian pulse to a CW field. Dashed line: incident field; solid line: transmitted field. Mean-filed theory, C = 20.0, γ/κ = 10.0, time in units of κ^{-1}.

(A) y_0 = 20.3, A = 1.0, $\hat{t}$ = 1.0

(B) y_0 = 20.3, A = 2.0, $\hat{t}$ = 2.0

(C) y_0 = 20.3, A = 1.0, $\hat{t}$ = 3.0

Figure 13 :

Minimum pulse width $\hat{t}_m$ as a function of the pulse amplitude A for various values y_0 of the CW laser field. Upper curve: y_0 = 20.8, middle curve: y_0 = 20.3, lower curve: y_0 = 19.6. The other parameters are C = 20, y_1 = 21, T_1 = 10, T_2 = 20, κ^{-1} = 1.

Figure 14 : Histogram of the tunneling times for t_c = 0.01, I = 25, and y_0 = 20.3. The other parameters are the same as in Fig. 13.

Table 1 :

Summary of numerical results: I = noise power, t_c = noise correlation time, $\langle t \rangle_{num}$ = numerical tunneling time, $\langle t \rangle_{th}$ = theoretical tunneling time, R_{num} = numerical tunneling times ratio, R_{th} = theoretical tunneling times ratio, N = number of computer runs. The relevant parameters are the same as for Fig. 13, and all the runs are for y_0 = 20.3.

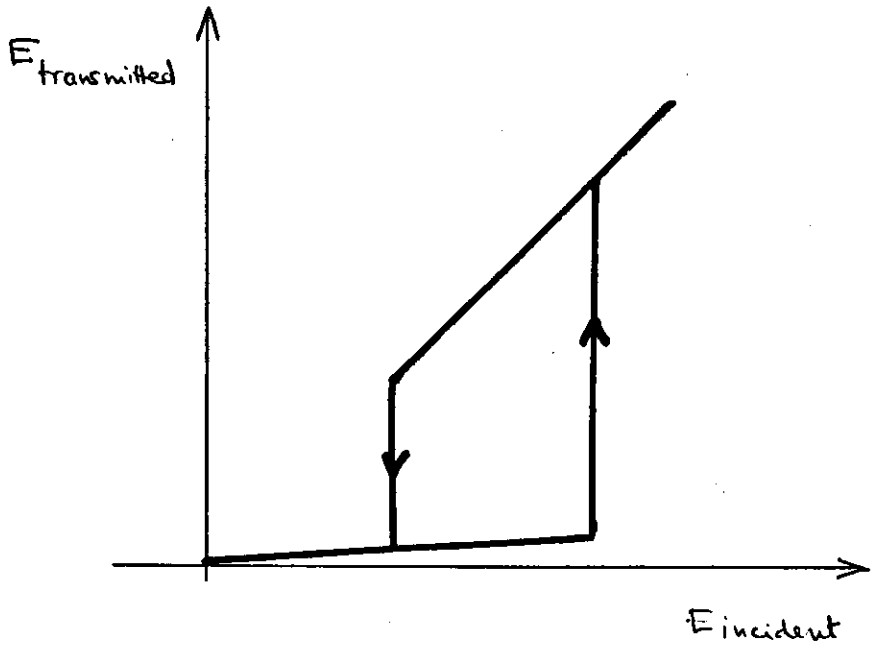

Figure 1

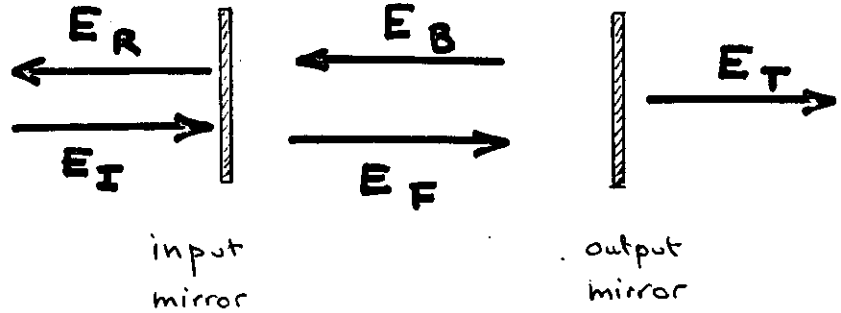

Figure 2

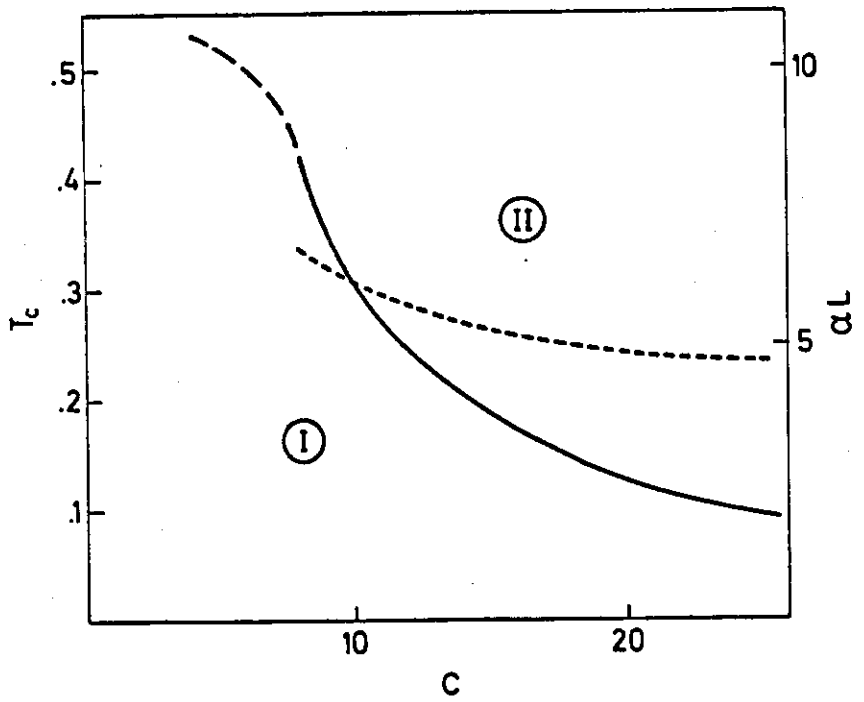

41

Figure 3

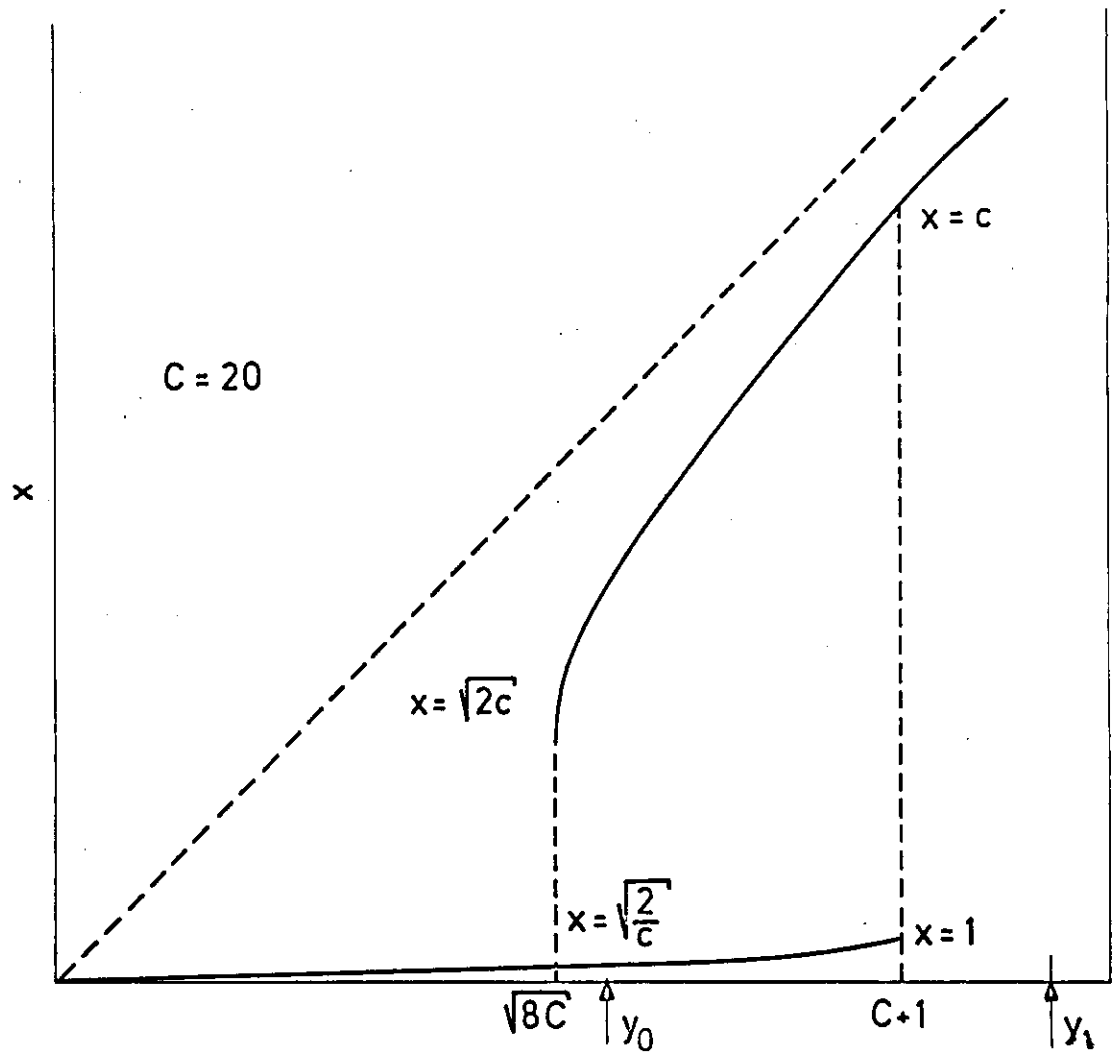

42

Figure 4

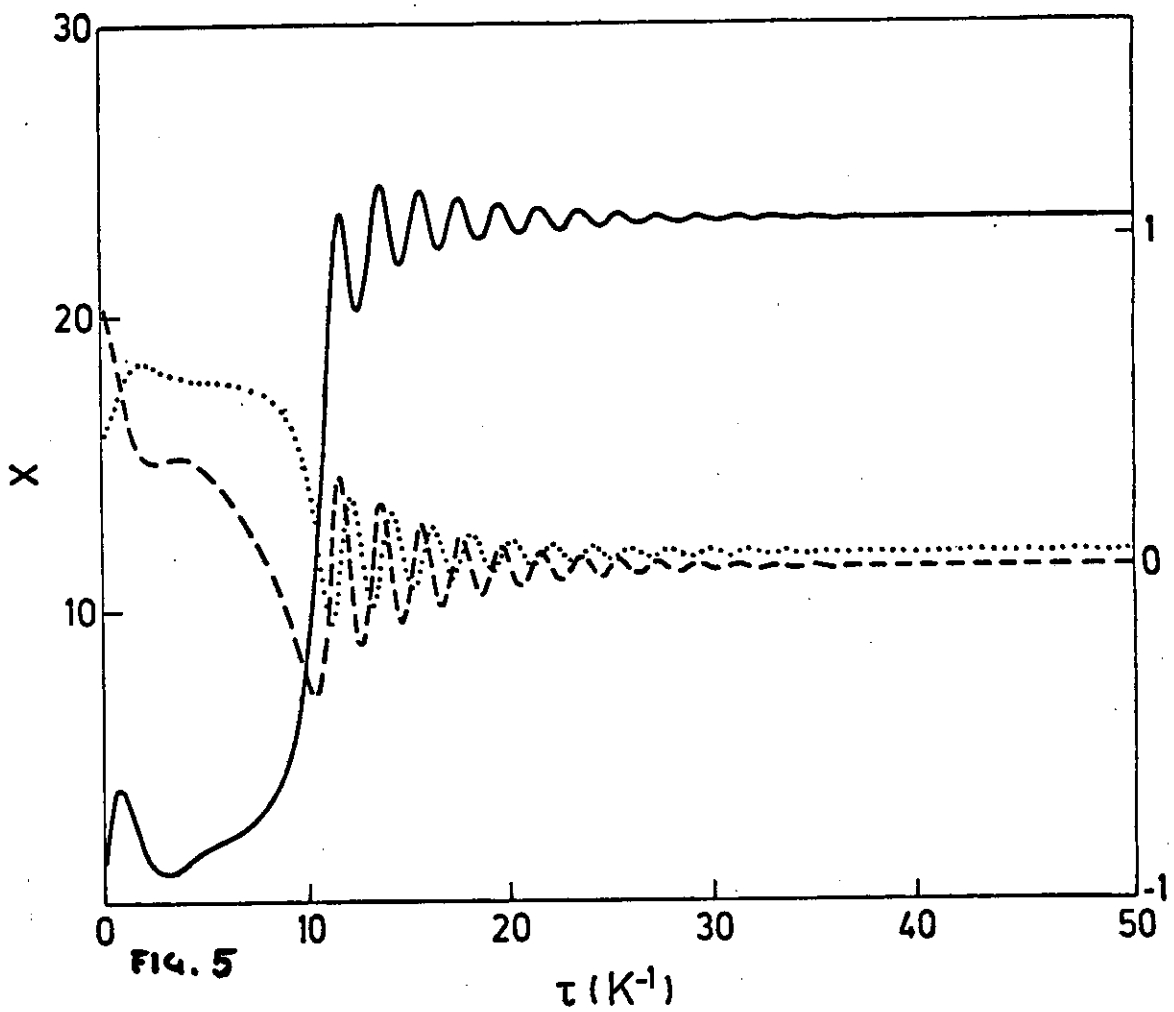

FIG. 5

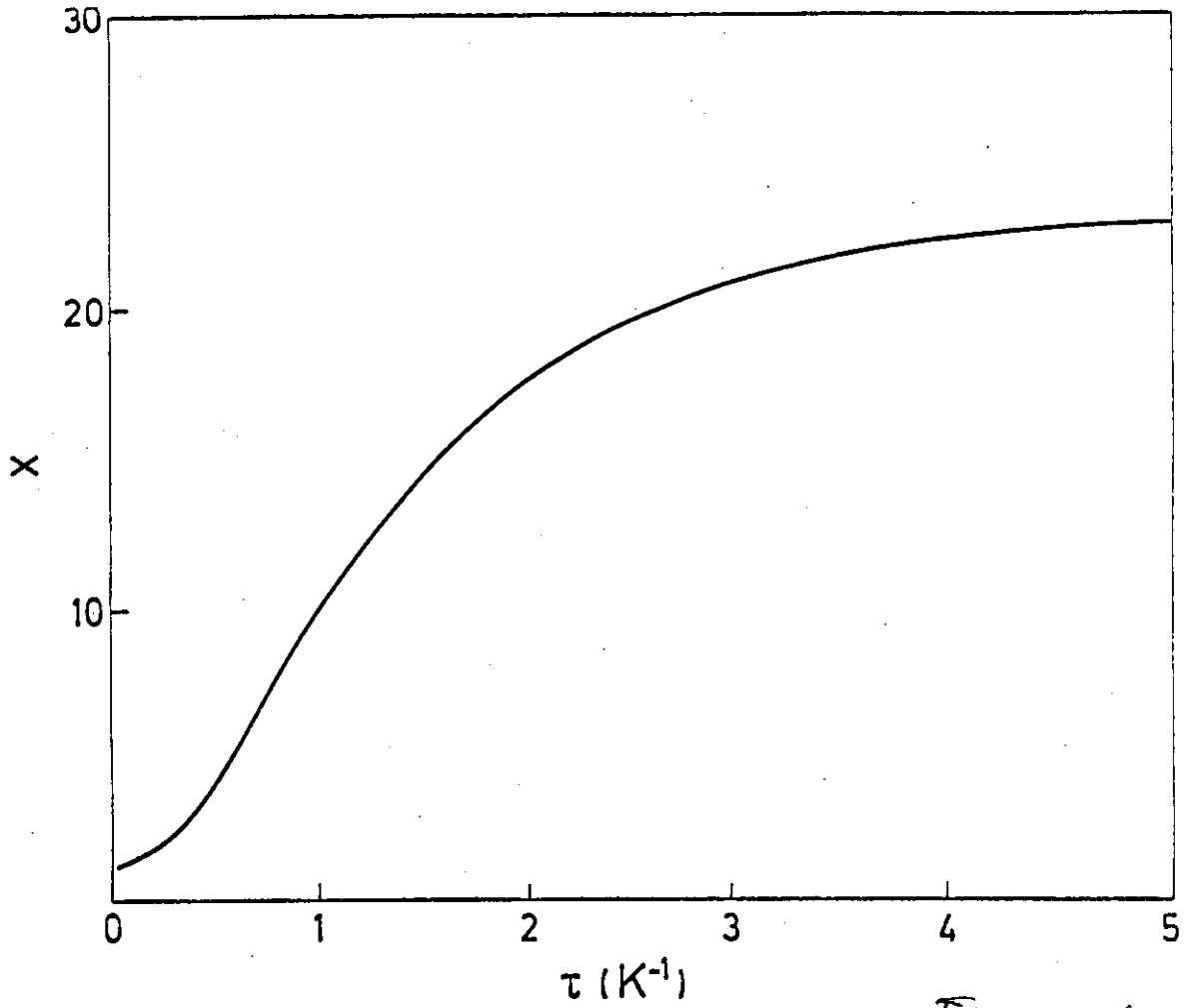

Figure 6

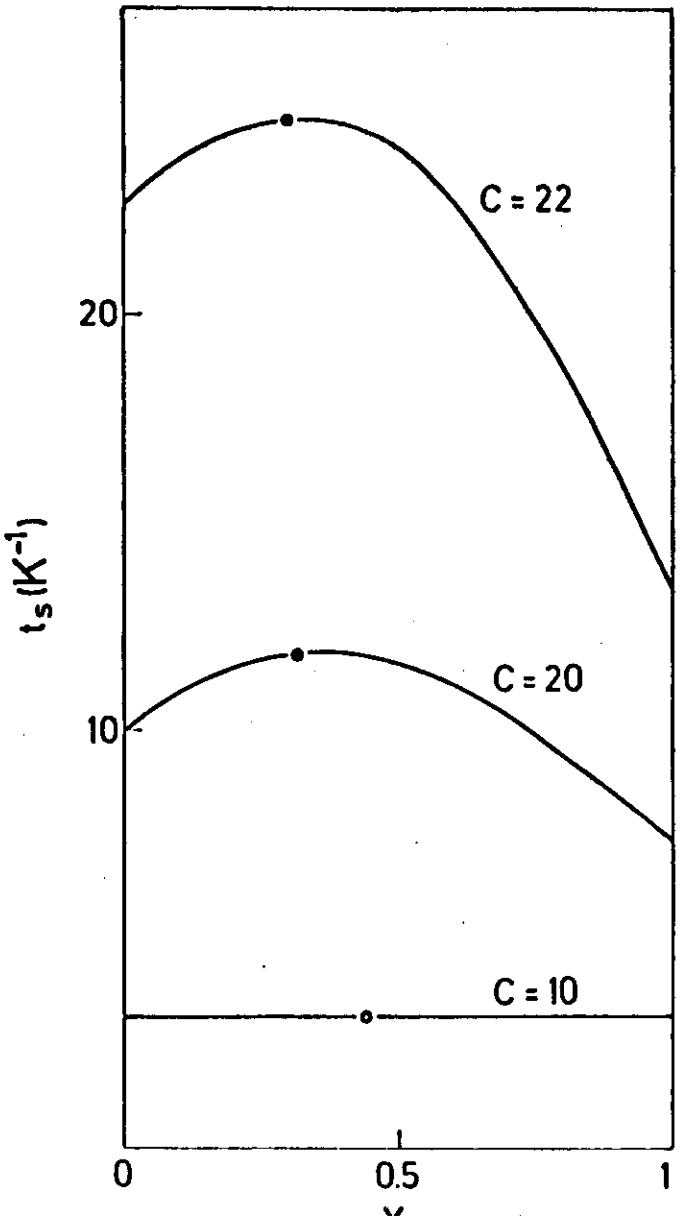

Figure 2

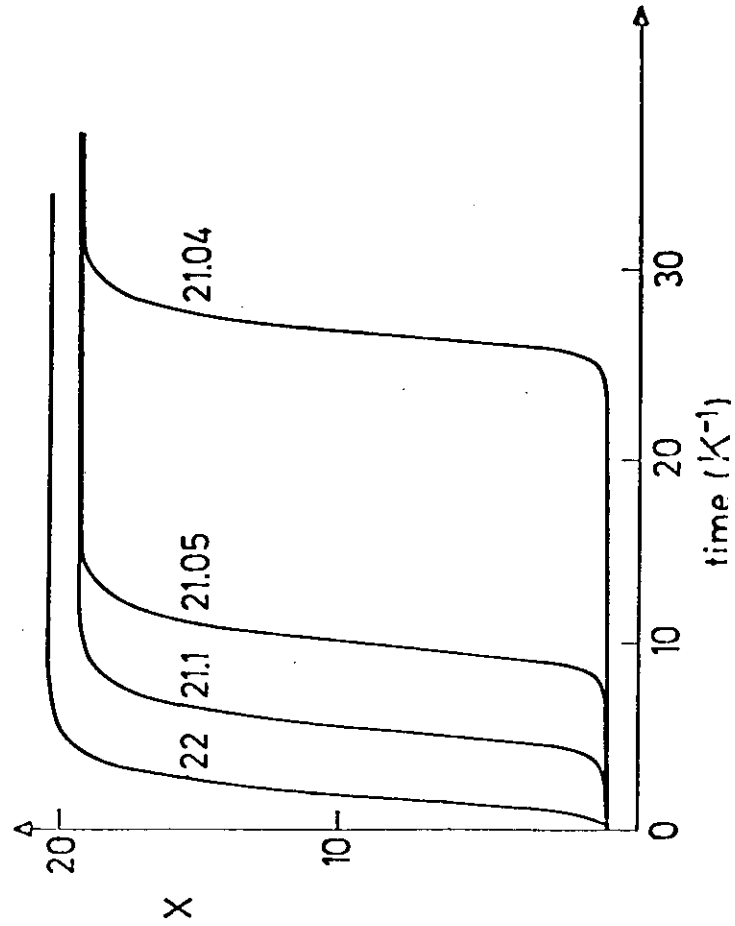

Figure 8

47

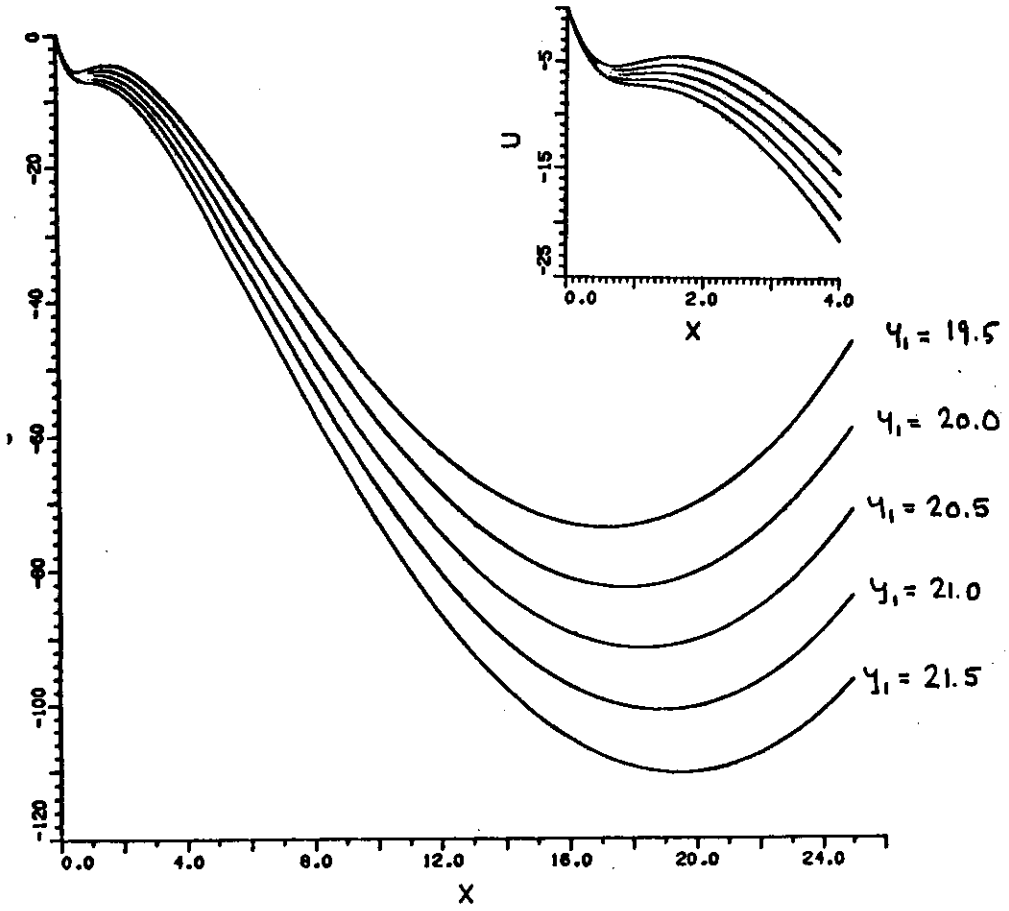

Figure 9

48

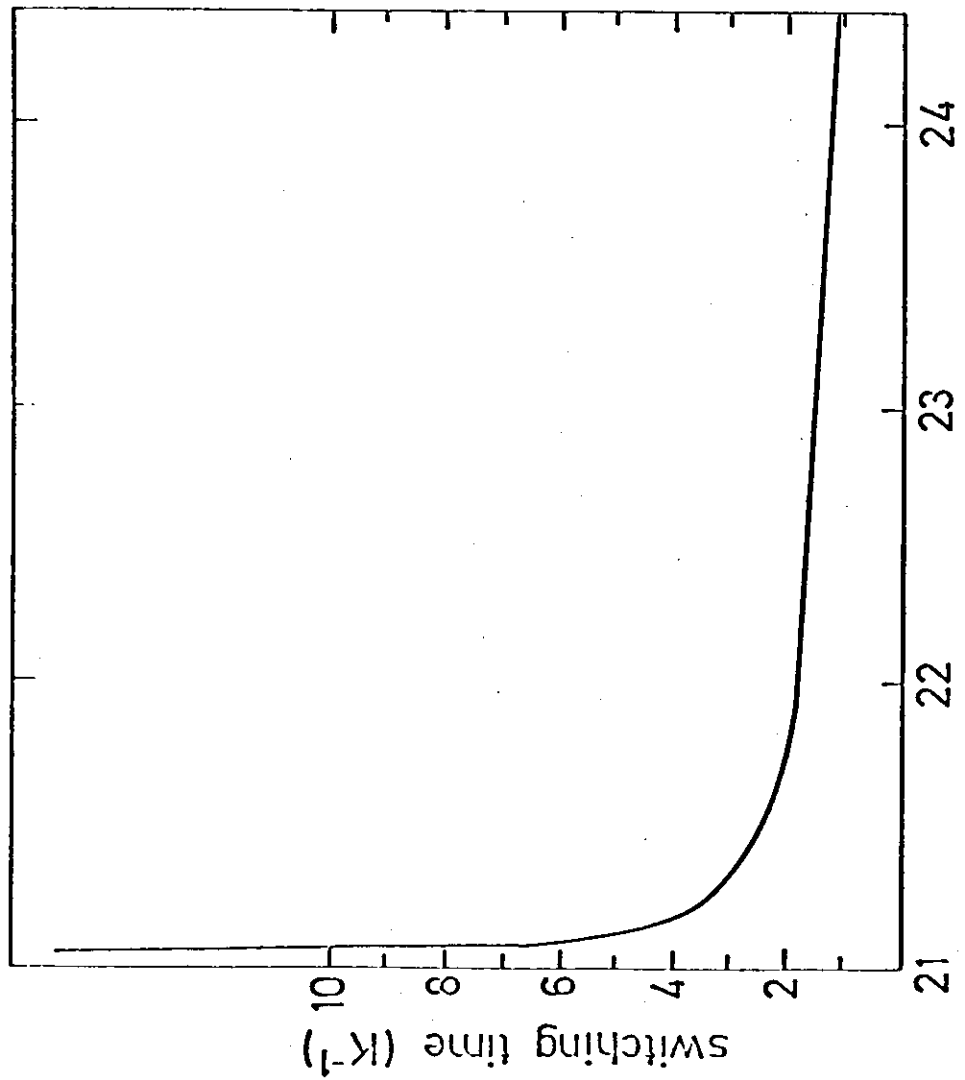

Figure 10

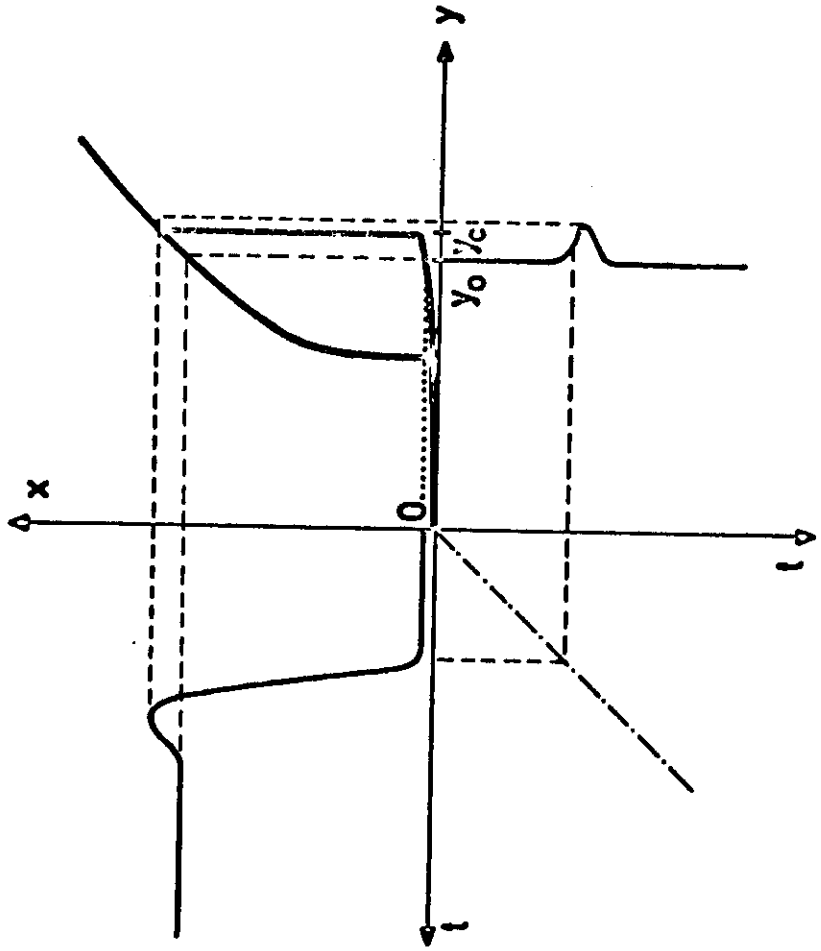
y
x
0
t
t
y_c
y_0

Figure 11

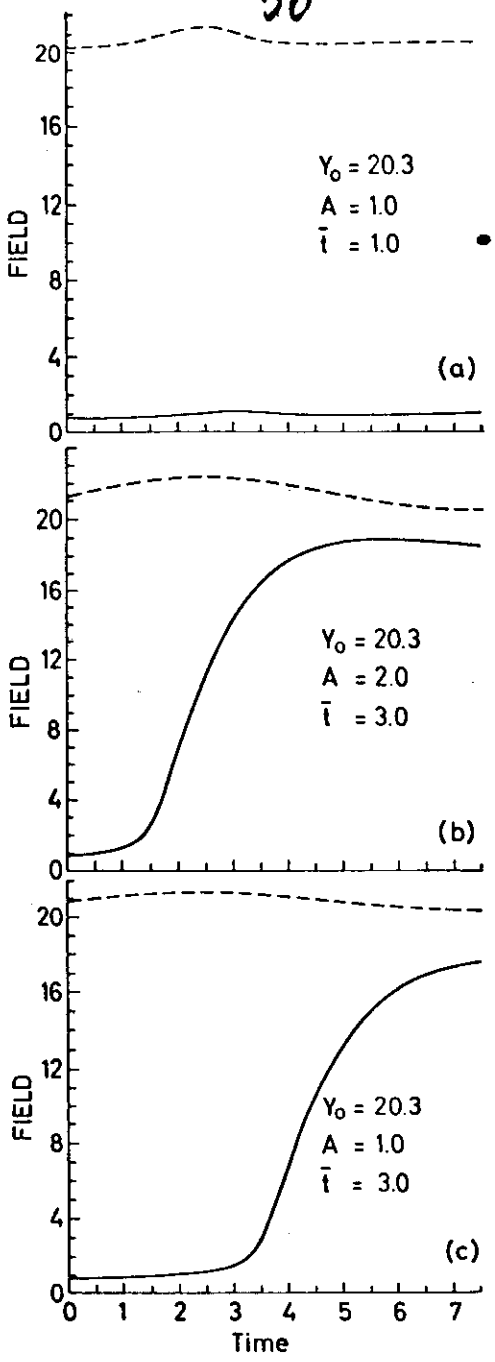
FIELD
Y_0 = 20.3
A = 1.0
$\bar{t}$ = 1.0
(a)
Y_0 = 20.3
A = 2.0
$\bar{t}$ = 3.0
(b)
Y_0 = 20.3
A = 1.0
$\bar{t}$ = 3.0
(c)
Time

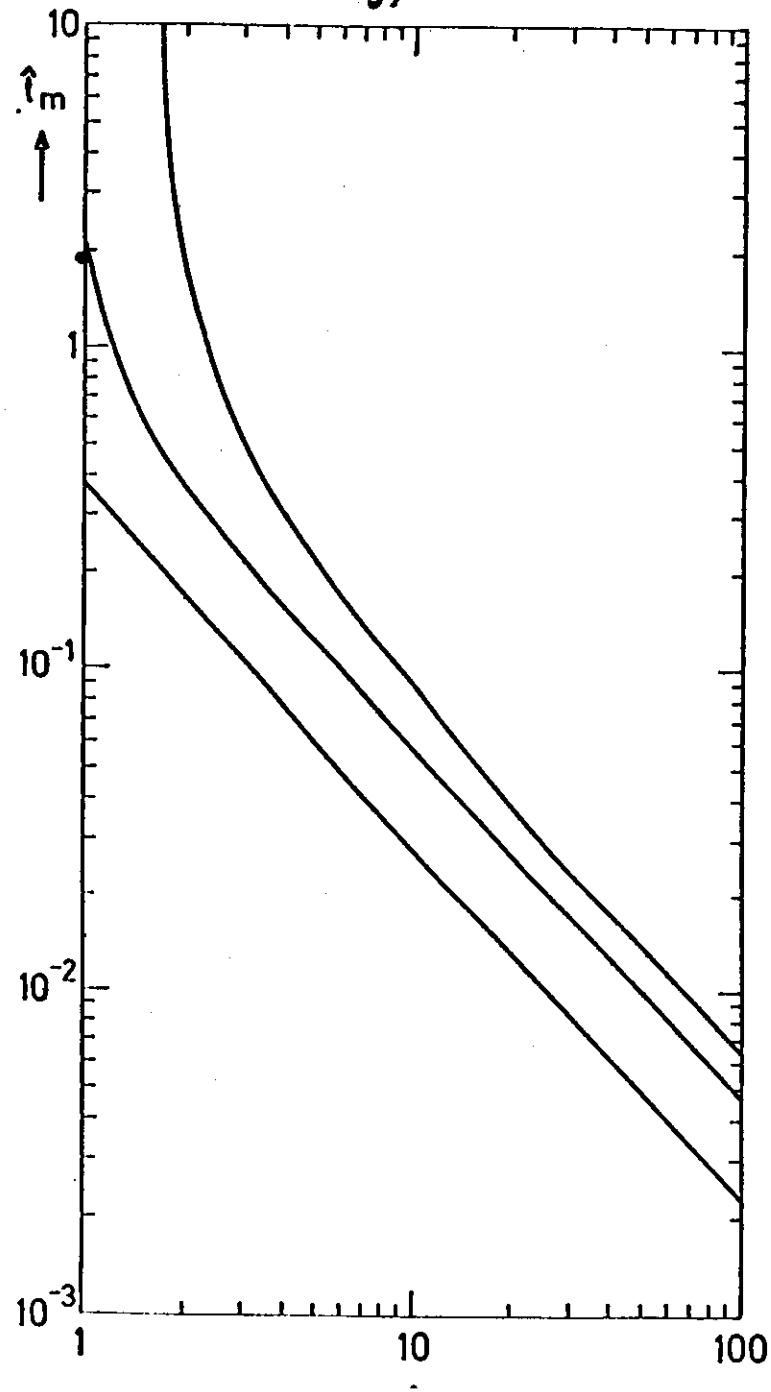
10
$\hat{t}_m$
1
10^{-1}
10^{-2}
10^{-3}
1
10
100

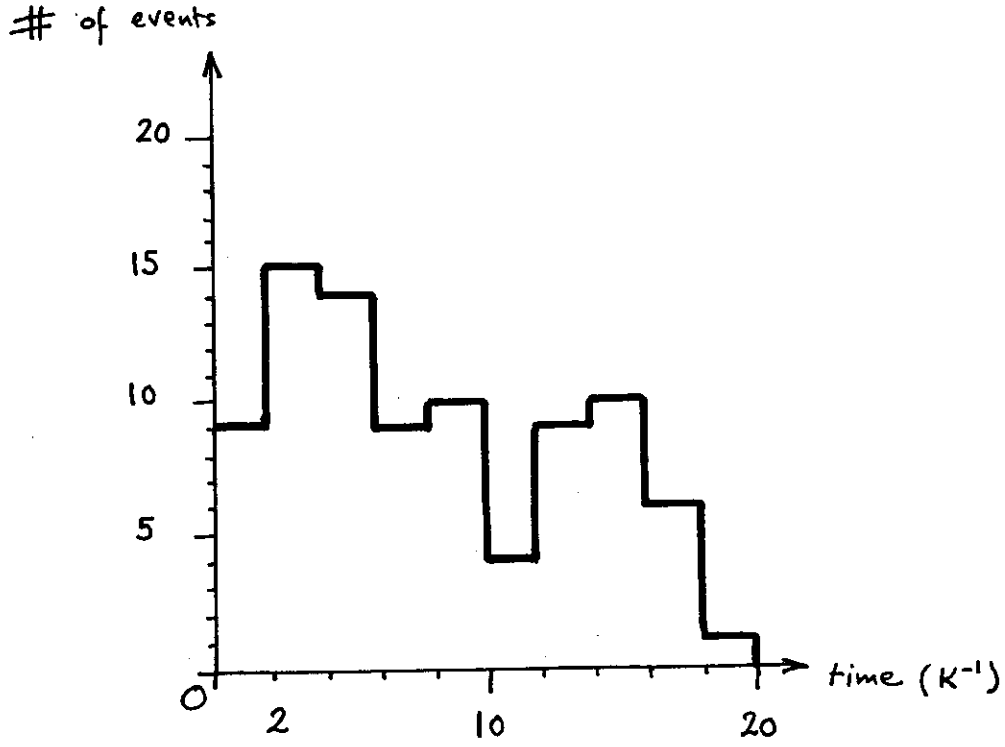
# of events
20
15
10
5
0
2
10
20
time (K^{-1})

Figure 14

t_c	I	$\langle t \rangle_{num}$	R_{num}	$\langle t \rangle_{th}$	R_{th}	N
10^{-2}	4.0	>100	>43	1.7×10^4	1.4×10^4	20
10^{-2}	16.0	41.0	17.83	11.5	9.58	12
10^{-2}	25.0	8.2	3.57	4.7	3.92	100
10^{-2}	100.0	3.2	1.39	1.5	1.25	10
10^{-1}	25.0	2.3	1	1.2	1	100

Table 1